INTER-NOISE 2006
3-6 DECEMBER 2006
HONOLULU, HAWAII, USA

Including the irregularities in the light-weight floor/ceiling model

Hyuck Chung[a]
Department of Mathematics
The University of Auckland
Private Bag 92019
Auckland, New Zealand

Colin Fox[b]
Department of Mathematics
The University of Auckland
Private Bag 92019
Auckland, New Zealand

ABSTRACT

Chung and Fox previously presented a mathematical/computational model giving good prediction of low-frequency vibration of light-weight timber based floor/ceiling structures (LTFS) made up of: upper plate, joist beams and ceiling. In that work the geometry of the structure was assumed known, and precise. Experimental data from mock-up LTFS validated that model. In this paper we present an augmentation of that model by including uncertainty in the placement and shape of the timber joists. We calculate the variability in vibration response in the low-frequency range by taking account of measurements of the bending and twisting of 301 timber beams. Although, the model was originally constructed for low-frequency vibration, its usefulness in the mid-frequency range (> 150Hz) is discussed. Earlier results showed that the rigidity of the connection between the upper plate and joist beams plays an important role in predicting resonance frequencies and vibration levels. We further consider these connection conditions in the presence of uncertainty.

1 INTRODUCTION

In this paper we extend the recent series of researches on the light weight timber based floor/ceiling structures (LTFS) by the authors and New Zealand scientists ([4,7]). A series of papers by Brunskog and Hammer ([1,2,3]) show the effects of cavity space and the joists in the LTFS. Craik ([5,6]) show the vibration propagation across junctions between flexible plate and beam. Our extensions over their models are, first: inclusion of slippage interaction between the plate and the joists, and second: inclusion of irregularities of the joist properties.

This paper examines the effects of irregularities in the components on the low- to mid-frequency vibrations. The irregularities considered here are the Young's modulus, the shape of the joists and the varying rigidity at the contact between the upper plate and the joists.

In order to cope with the real life structures, the model must be able to incorporate the changes without going through the modelling procedure again. For this reason we chose the variational formulation of the system. The solution, in this case the deflection of the components, is the minima of the total energy in the structure. We show how to incorporate the interaction conditions between components, using the floor/ceiling configuration shown in figure 1.

[a] Email address: hyuck@math.auckland.ac.nz
[b] Email address: fox@math.auckland.ac.nz

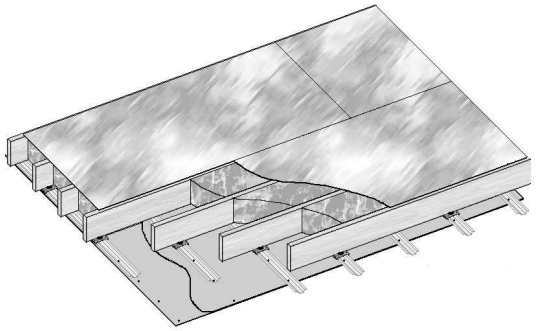

Figure 1. Schematic drawing of an example of the LTFS.

2 RESULTS FROM DETERMINISTIC MODEL

The authors ([4,7]) have shown that the deterministic model can predict the vibration (shape of the root mean squared velocity) well at a frequency range lower than 80Hz. An examples of the comparison of the root mean squared velocity between the modelling and the experiment results is shown in figure 2. The dimension of the structure is 7m by 3.2m. The joists are running in the lengthwise direction.

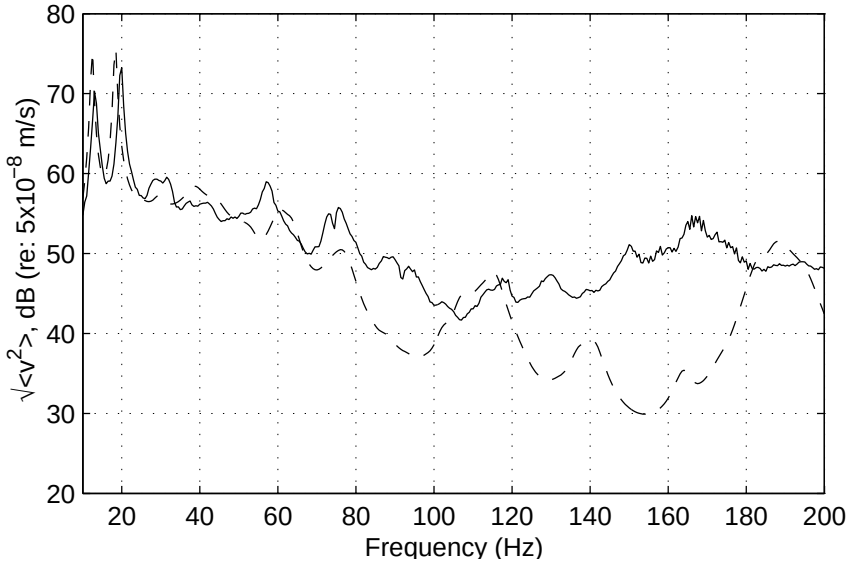

Figure 2. Comparison of the root mean squared velocity of the experimental (solid) and the theoretical (dashed) results from the structure in figure 1.

3 FORMULATION

3.1 Fourier expansion of vibration

The Fourier expansion method is chosen because of the regularity of the shape of the structure, in this case a rectangle. Furthermore so-called mounting condition for common floor/ceiling structures is *simply supported*. The deflection of the upper plate, ceiling and joists are expanded as follows,

$$w_i(x,y) = \sum_{m,n=1}^{N} c_{mn}^{i} \phi_m(x) \psi_n(y),\ i = 0, 2 \tag{1}$$

$$w_1(x,j) = \sum_{m=1}^{N} c_{mj}^{1} \phi_m(x),\ j = 1, 2, ..., S_j, \tag{2}$$

where

$$\phi_m(x) = \sqrt{\frac{2}{A}} \sin k_m x,\ \psi_n(y) = \sqrt{\frac{2}{B}} \sin \kappa_n y,\ \text{for } m, n = 1, 2, ..., N$$

and $k_m = \pi m / A$, $\kappa_n = \pi n / B$.

The acoustic pressure in the cavity is expressed by Helmholtz equation. Therefore the acoustic pressure can expanded by the Fourier cosine series in the (x,y) plane because the walls of the cavity is assumed to be acoustically hard. By solving the Helmholtz equation using the separation of variables, acoustic pressure $p(x,y,z)$ can be expanded as

$$p(x,y,z) = \sum_{m,n=0}^{N} \left(\Gamma_{mn}^{(1)} e^{\gamma_{mn} z} + \Gamma_{mn}^{(2)} e^{-\gamma_{mn} z} \right) \alpha_m(x) \beta_n(y)$$

where $\gamma_{mn} = (k_m{}^2 + \kappa_n{}^2 - k^2)^{0.5}$ and $k = \omega / c$, c being the speed of sound. The modes are

$$\alpha_m(x) = \sqrt{\frac{2}{A}} \cos k_m x,\ \beta_n(x) = \sqrt{\frac{2}{B}} \cos \kappa_n y,\ \text{for } m, n = 0, 1, ...N$$

3.2 Energy of the components

We derive the variational formulation of the whole structure with respect to the vectors of the Fourier coefficients of each component. This formulation procedure enables one to change the configuration of the structure because the apparent form of the resulting equations stay unchanged.

The strain energy and the kinetic energy of a Kirchhoff plate ([8]) is given by

$$\frac{1}{2} \int_0^A \int_0^B \left\{ D \left[\left(\nabla^2 w \right)^2 + 2(1-\nu) \left(w_{xx} w_{yy} - w_{xy}^2 \right) \right] - m\omega^2 w^2 \right\} dx dy,$$

and for an Euler beam we have

$$\frac{1}{2} \int_0^A \left\{ EI w_{xx}^2 - m\omega^2 w^2 \right\} dx \tag{3}$$

where w, D, E, I and m are vertical deflection, flexural rigidity, Young's modulus, moment of inertia (of the beam) and mass density, respectively.

The strain energy of the plates and the beams can be expressed using the vectors of the coefficients of the expansion given by equations 1 and 2,

$$\pi_i = \frac{1}{2} \mathbf{c}_i^{\mathrm{t}} M_i \mathbf{c}_i,\ i = 0, 1, 2,$$

where the index i=0,1,2 indicates the upper plate, the joists and the ceiling, respectively. Note that the matrices M_i are diagonal.

We consider the joist beams that are in contact with the upper plate. The deflection of the joists is exactly same as the upper plate, which leads to the following relationship between $\mathbf{c}_0$ and $\mathbf{c}_1$.

$$\mathbf{c}_1 = L\mathbf{c}_0 \tag{4}$$

where matrix L represents the following summation

$$\sum_{n=1}^{N} c_{mn}^{0} \psi_n(y_j),\ j = 1, 2, ..., S_1.$$

The ceiling is normally attached to the joists by rubber clips that are designed to isolate the vibration of the joists. The potential energy of the rubber connectors is

$$\frac{\tau}{2} \sum_{i,j} \{w_1(x_i, j) - w_2(x_i, y_j)\}^2$$

where τ is the spring constant of the rubber connector located at (x_i, y_j).

3.3 Inclusion of irregularity

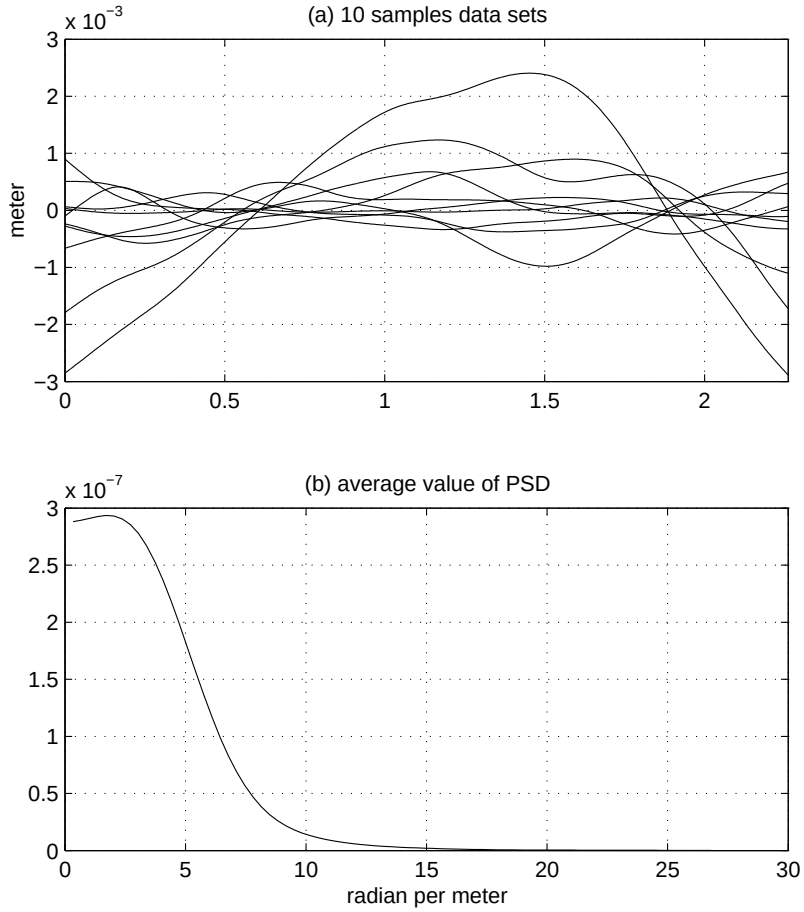

Figure 3. (a) 10 samples of the measurements of the timber shape. (b) average of the power spectra density of the timber shape.

The irregularities considered here are three, which are contact rigidity, joist's Young's modulus and shape of the joists. The irregularities are defined as the deviation from the ideal constant value. We denote the parameters by

$$\theta(x, j), \text{ joist shape}$$
$$\sigma_0 + \sigma(x, j), \text{ contact regidity}$$
$$\varepsilon_0 + \varepsilon(x, j), \text{ Young's modulus}$$

Note that the mean of the above deviations is zero. The above irregularity functions can be characterised using their power spectral density (PSD), for example the PSD of $\sigma(x,j)$ is

$$S_{\theta\theta}(\xi) = \lim_{T\to\infty} \frac{1}{2T} \left| \hat{\theta}(\xi) \right|^2$$

where $\hat{\sigma}(\xi)$ is the Fourier transform of σ and T is the sampling period (see [9]). In the remainder of this subsection, the irregularities are incorporated for the given PSD, $S_{\sigma\sigma}(\xi)$ and $S_{\varepsilon\varepsilon}(\xi)$.

The measurement data of the 301 dry pine beams that is currently available to the authors is shown in figure 3 as the average of the PSD. Ten examples of measurements are also shown. The dimension of the beams is approximately 0.1m by 0.2m and the length is 2.4m. The PSD in figure 3 indicates that the beams have mostly two or three twists or four at the most.

3.3.1 Joist shape

The deviation θ gives curves instead of straight lines for the contact between the upper plate and the joists. We first take the Taylor expansion of the vibration modes at the contact curves and omit the higher terms because θ is small.

$$\begin{aligned} \psi_n\left(y_j + \theta(x, j)\right) &= \sum_{i=0}^{\infty} \frac{\left(\kappa_n y_j \theta(x, j)\right)^i}{i!} \frac{d^i \psi_n}{dy^i}\left(y_j\right) \\ &\approx \psi_n\left(y_j\right) + \kappa_n^2 y_j \theta(x, j) \beta_n\left(y_j\right) \end{aligned} \tag{5}$$

Note that the first term leads to the zero deviation solution given from the contact condition equation 4.

The above expansion leads to the following modified contact condition.

$$\sum_{m=1}^{N} c_{mj}^1 \phi_m(x) = \sum_{m,n=1}^{N} c_{mn}^0 \phi_m(x) \psi_n\left(y_j + \theta(x, j)\right)$$

Using the orthogonal relationship and equation 5 gives

$$\begin{aligned} c_{mj}^1 &= \sum_{m,n=1}^{N} c_{mn}^0 \psi_n\left(y_j\right) \\ &\quad + \sum_{m',n}^{N} q_{nj} c_{m'n}^0 \int_0^A \theta(x, j) \phi_m(x) \phi_{m'}(x) dx \end{aligned} \tag{6}$$

where $q_{nj} = \kappa_n^2 y_j \beta_n\left(y_j\right)$. Hence we rewrite the above equation with matrix notations.

$$\mathbf{c}_1 = \left[L + L_\theta\right] \mathbf{c}_0.$$

The elements of matrix L_θ can be better visualised by rewriting the formula using the convolution of the Fourier transform. Then the elements of L_θ are computed by

$$q_{nj}\left[\hat{\theta} * \widehat{H} * \left\{\delta\left(k_m - k_{m'}\right) - \delta\left(k_m + k_{m'}\right)\right\}\right] \tag{7}$$

where * is the convolution. $\widehat{H}(\xi)$ is the Fourier transform of rectangular pulse in [0,A],

$$\widehat{H}(\xi) = \frac{\mathrm{i}}{\xi}\left(e^{\mathrm{i}A\xi} - 1\right)$$

Figure 4 shows illustration of the above convolutions. These timber beams are not intended for the floor/ceiling structures as they have many twists and turns. However, if we were to use the data in our 7 meter long LTFS, figure 4 tells us that we would have to compute higher order off-diagonal terms in L_θ in order to capture the irregularity.

We rewrite the above formula so that the deviation part can appear as additive terms to the regular term. The potential energy contribution from the beams is then

$$\pi_1 = \frac{1}{2}\mathbf{c}_1^{\mathrm{t}} M_1 \mathbf{c}_1 = \frac{1}{2}\mathbf{c}_0^{\mathrm{t}}\left(L + L_\theta\right)^{\mathrm{t}} M_1 \left(L + L_\theta\right)\mathbf{c}_0$$

Higher order terms may be used when more details of the shape deviation have to be included. When only the first order terms are used, the deviation parts become simple additive terms to the deterministic parts.

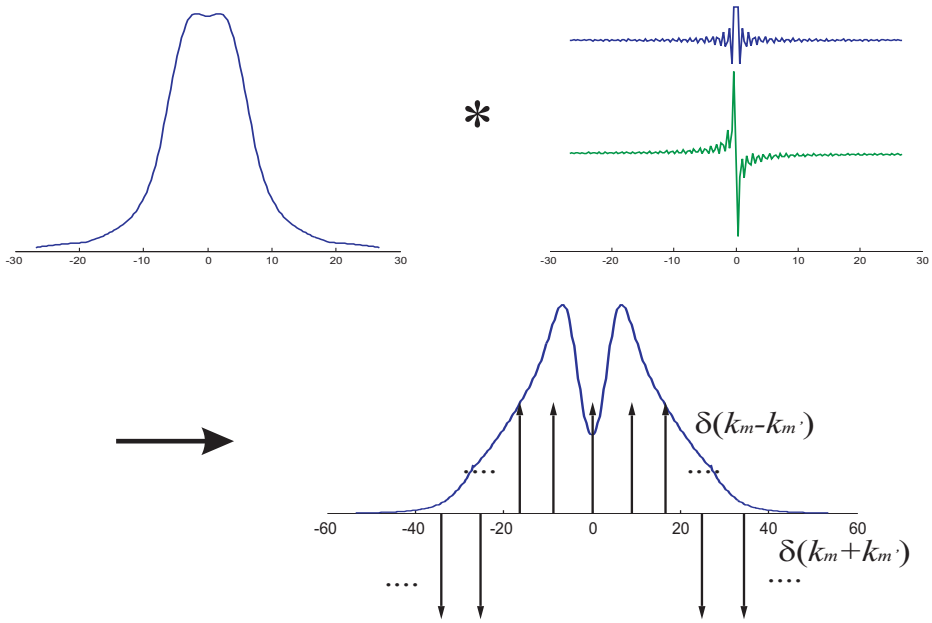

Figure 4. Illustration of the convolution in equation 7, i.e., $\hat{\theta} * \widehat{H}$. The delta functions are depicted as arrows in the third figure.

3.3.2 Joist Young's modulus

The Young's modulus deviation ε can be incorporate using the similar procedure given for θ. The strain energy of the joist beam is

$$\frac{I}{2}\int_0^A \left(\varepsilon_0 + \varepsilon(x,j)\right)\left\{\frac{d^2 w_1}{dx^2}(x,j)\right\}^2 dx$$

where I is the moment of inertia. Again the deviation is expressed by the power spectral density,

$$S_{\varepsilon\varepsilon}(\xi) = \lim_{T\to\infty}\frac{1}{2T}\left|\hat{\varepsilon}(\xi)\right|^2$$

where $\hat{\varepsilon}$ is the Fourier transform of ε.

Using the expansion of w_1 and ε gives

$$\frac{1}{2}\mathbf{c}_1^{\mathrm{t}}\left\{M_1 + L_\varepsilon\right\}\mathbf{c}_1$$

where the elements of L_ε are derived by

$$Ik_m k_{m'}\int_0^A \varepsilon(x,j)\phi_m(x)\phi_{m'}(x)dx$$

Rewriting the integral part of this equation in the similar manner shown in equation 7 gives

$$Ik_m k_{m'}\left[\hat{\varepsilon} * \widehat{H} * \left\{\delta(k_m - k_{m'}) - \delta(k_m + k_{m'})\right\}\right] \tag{8}$$

3.3.3 Contact rigidity

The potential energy due to the slippage resistance is

$$\frac{1}{2}\sum_{j=1}^{S_1}\int_0^A \left(\sigma_0 + \sigma(x,j)\right)\left(\frac{H}{2}\frac{dw_1}{dx}(x,j)\right)^2 dx$$

where $H = h_0 + h_1$.

The resulting energy is also written using the matrices and the vectors of the coefficients.

$$\frac{1}{2}\mathbf{c}_1^{\mathrm{t}} N_s \mathbf{c}_1.$$

Matrix N_s can be decomposed into the following deterministic and deviation parts.

$$N_s = N + L_\sigma$$

where the elements of L_σ are derived from the following integrals

$$k_m k_{m'}\left[\widehat{\sigma} * \widehat{H} * \left\{\delta(k_m - k_{m'}) + \delta(k_m + k_{m'})\right\}\right]$$

The deterministic matrix N is a diagonal matrix of $\sigma_0 H^2 {k_m}^2/4$.

3.4 Acoustic pressure in the cavity

The acoustic pressure and the plates are coupled by the Neumann conditions at z=0, h,

$$\left.\frac{\partial p}{\partial z}\right|_{z=0} = \rho\omega^2 w_0(x,y),\ \left.\frac{\partial p}{\partial z}\right|_{z=h} = \rho\omega^2 w_2(x,y),$$

where ρ is the mass density of the cavity air. The above conditions give the relationship between $\mathbf{c} = (\mathbf{c}_0, \mathbf{c}_2)$ and $\boldsymbol{\Gamma}$ (vector of ${\Gamma_{\mathrm{mn}}}^{(1)}$ and ${\Gamma_{\mathrm{mn}}}^{(2)}$)

$$Q_a \boldsymbol{\Gamma} = \rho\omega^2 \mathbf{c}$$

where the matrix Q_a is derived from the integrals of the products of the basis functions,

$$\int_0^A \int_0^B \phi_m(x)\psi_n(y)\alpha_{m'}(x)\beta_{n'}(y)dxdy$$

The contribution from the air pressure must be added to the equations for the plates. Then we have,

$$M_p \mathbf{c} = Q_p \mathbf{\Gamma} + \mathbf{F}$$

where the excitation vector **F** is given by

$$F_0 \phi_m (x_0) \psi_n (y_0),\ m,n = 1,2,...,N$$

where (x_0,y_0) is the location of the excitation and F_0 is amplitude of the force.

Hence the vectors $\mathbf{c}_0$ and $\mathbf{c}_2$ can be computed from

$$\begin{pmatrix} M_p & -Q_p \\ \rho\omega^2 I & -Q_a \end{pmatrix} \begin{pmatrix} \mathbf{c} \\ \mathbf{\Gamma} \end{pmatrix} = \begin{pmatrix} \mathbf{F} \\ 0 \end{pmatrix} \tag{9}$$

where I is an identity matrix.

In order to include the irregularities, we simply have to modify M_p in equation 9 to

$$M_p + L_\theta + L_\varepsilon + L_\sigma$$

3.5 Additional components

Here briefly demonstrate how additional components can be incorporated into the model. The structure depicted in figure 1 has additional ceiling batten attached to the ceiling. These battens can be added to the model by following the same way how the joists were attached to the upper plate. Let $\mathbf{c}_3$ denote the vector of the coefficients of the additional components, which are now expanded over $\{\psi_n\}$. Therefore we have an equivalent contact condition to equation 4. Only this time the matrix represents the following summation.

$$\sum_{m=1}^{N} c_{mn}^2 \phi_m (x_i),\ i = 1,2,...,S_2,$$

where S_2 is the number of battens and x_i is the location of the batten. The strain energy of the battens,

$$\pi_3 = \frac{1}{2} \mathbf{c}_3^{\mathrm{t}} M_3 \mathbf{c}_3$$

can now be added to the total energy formula as shown in section 3.2.

4 SUMMARY

We have shown how the irregularities in the components of the light-weight floor/ceiling structures can be included in the theoretical model. The irregularities are represented by the deviation from the expected values. The deviation is then incorporated into the solution formulae as the PSD as shown in figure 2. The shape of the PSD intuitively illustrates how many off-diagonal elements are needed to represent the irregularity in the system of equations 9. The most notable advantage of the method of solution is that the formulae remain unchanged regardless of the complexity of the structure.

ACKNOWLEDGEMENTS

H. Chung acknowledges New Zealand Science and Technology Foundation post-doctoral fellowship (Contract number: UOAX0505). Figure 1 is courtesy of G. Schmid of the Acoustics Research Centre.

REFERENCES

[1] J. Brunskog and P. Hammer, “Models to predict impact sound transmission of lightweight floors, A Literature survey,” Journal of Building Acoustic, Volume 7, number 2, (2000).

[2] J. Brunskog and P. Hammer, “Acoustic properties of resilient, statically tensile loaded devices in lightweight structures: A measurement method and statistical analysis,” Journal of Building Acoustic, Volume 9, number 2, pp. 99 - 137 (2002).
[3] J. Brunskog and P. Hammer, “Prediction model for the impact sound level of lightweight floors,” Acta Acustica united with Acustica, Volume 89, pp. 309-322 (2003).
[4] H. Chung and G. Emms, “Fourier series solutions to the vibration of rectangular light-weight floor/ceiling structures,” ACTA Acustica (submitted 2006)
[5] R.J.M. Craik and R.S. Smith, “Sound transmission through lightweight parallel plate. part II: Structure-borne sound,” Applied Acoustics, 61, pp.247--269 (2000).
[6] R.J.M. Craik and R.S. Smith, 2000, “Sound transmission through double leaf lightweight partitions part I: Air-borne sound,” Applied Acoustics, 61, pp.223--245.
[7] G. Emms, H. Chung, G. Dodd, G. Schmid, and K. McGunnigle, “FWPRDC Project PN04.2005 Maximising impact sound resistance of timber framed floor/ceiling systems,” The Forest and Wood Products Research and Development Corporation. Australian Government, www.fwprdc.org.au (2006)
[8] F.S. Fahy, “Sound and Structural Vibration,” Academic Press Ltd. London, (1985).
[9] M.K. Ochi, “Applied probability and stochastic processes in engineering and physical sciences,” John Wiley and Sons, New York, 1990.*American National Standard Acoustical Terminology*, American National Standards Institute ANSI S1.1-1994 (Acoustical Society of America, New York, 1994).